Chapter 20
Assessment of the Seismic Response of Concentrically-Braced Steel Frames

Brian M. Broderick, Jamie Goggins, Darko Beg, Ahmed Y. Elghazouli, Philippe Mongabure, Alain Le Maoult, Alan Hunt, Suhaib Salawdeh, Primoz Moze, Gerard O'Reilly and Franc Sinur

20.1 Introduction

Concentrically braced frames (CBFs) offer an economical and efficient form of earthquake resistance for steel structures. For small, more frequent earthquakes, they provide sufficient stiffness and strength to meet serviceability requirements. For larger earthquakes, adequate seismic design and detailing can ensure a dissipative response that limits structural response. Diagonal bracing members CBFs are critical elements that during severe seismic loading experience repeated cycles involving yielding in tension and member buckling in compression. The performance of these members depends on various factors, including local slenderness, global slenderness, material yield strength, section shape and end restraint (Elghazouli 2003).

Due to the difficulty in accurately modelling their complex seismic response, numerous experimental studies have been carried out to study the cyclic inelastic behaviour of bracing members. Early studies examined the load-displacement

B. M. Broderick (✉) · A. Hunt
Department of Civil, Structural and Environmental Engineering,
Trinity College, Dublin, Ireland
e-mail: bbrodrck@tcd.ie

J. Goggins · S. Salawdeh · G. O'Reilly
College of Engineering and Informatics, National University of Ireland, Galway, Ireland

D. Beg · P. Moze · F. Sinur
Faculty of Civil and Geodetic Engineering, University of Ljubljana, Ljubljana, Slovenia

A. Y. Elghazouli
Department of Civil and Environmental Engineering, Imperial College, London SW7 2AZ , UK

P. Mongabure · A. Le Maoult
CEA Saclay, DEN/DANS/DM2S/SEMT/EMSI, 91191 Gif sur Yvette Cedex, France

F. Taucer, R. Apostolska (eds.), *Experimental Research in Earthquake Engineering,*
Geotechnical, Geological and Earthquake Engineering 35,
DOI 10.1007/978-3-319-10136-1_20

hysteretic response which was shown to be most strongly influenced by global slenderness (Popov and Black 1981). Slender members lost compressive resistance more rapidly than stocky members, resulting in fewer inelastic response cycles and less energy dissipation. More recently, attention has shifted to examination of the factors influencing the fracture life of bracing members. Through experimental testing, both global and local slenderness were found to influence fracture life (Tremblay 2002), and empirical expressions for the fracture life and ductility capacity of hollow section bracing members have been proposed (Goggins et al. 2006; Nip et al. 2010).

Gusset-plate connections employed in CBFs in which out-of-plane brace buckling is envisaged must be designed to accommodate the large brace end-rotations experienced at large storey drifts. This implies the formation of a stable ductile plastic hinge within the gusset plate. The design details must also prevent gusset plate buckling in compression or yielding in tension (AISC 2005). However, current design guidance and practice can lead to the use of over-sized gusset plates which reduce the seismic performance of the brace members themselves. More recently, balanced gusset plate detailing rules have been recommended, which result in more efficient connection designs while improving the seismic performance of the CBF overall (Lehman et al. 2008).

20.2 Experimental Aims and Methodology

20.2.1 Research Objectives

The overall aim of the BRACED project was to improve the understanding of, and numerical modelling methods for, steel CBFs subjected to seismic loading; and to assess the implications for design methods and guidance. This is achieved by addressing three principal objectives:

- A large body of research has generated theoretical and empirical formulae to predict key brace member performance parameters for earthquake response. These include the stiffness, resistance and ductility of individual brace members and whole CBFs. The BRACED project examines the validity of these predictive formulae under realistic dynamic response conditions using shake table testing of model CBFs, supported by complementary quasi-static cyclic testing and numerical modelling.
- More recent research has shown that standard practice in brace connection design can be improved by using alternative geometrical details. This project assesses the influence of different gusset plate designs on the dynamic response of CBFs to earthquake ground motion.
- Finite element software has been used in engineering research and practice to model the global response of braced frames and the local response of brace members and brace connections. In this project, OpenSees modelling techniques

proposed for this form of structure will be investigated, and the software's ability to model the earthquake response of CBFs will be validated through correlation with test results.

20.2.2 Methodology

The BRACED Project was initiated as part of the Transnational Access programme offered by the European Commission's Seventh Framework Programme (FP7) project SERIES (Seismic Engineering Research Infrastructures for European Synergies). The main experimental phase was carried out at the TAMARIS Laboratory in the Laboratoire d'Etudes de Mécanique Sismique (EMSI) at CEA Saclay, France. The tests were carried out on the AZALEE shake table. The AZALEE platform has an area of 6×6 m and can accommodate test masses up to 100 t. It is capable of triaxial excitations up to 1.0 g, offering six degrees of freedom and maximum longitudinal and lateral displacement of ± 125 mm.

These series of shake table tests investigated the ultimate behaviour of CBFs through shake table testing of a model test frame incorporating pairs of brace specimens with different brace member and gusset plate characteristics. The seismic performance of such structures during strong earthquakes can be affected by the limited ductility capacity of brace members under low cycle fatigue conditions. The experimental programme was designed to assess whether existing models for evaluating the ductility capacity of hollow section bracing members (which were generally developed using quasi-static cyclic test results) capture observed behaviour during dynamic response conditions. Hence the test programme examines brace members with different cross-section sizes, and therefore different global and local slendernesses. Recent proposals for improved design and detailing guidance for gusset plate connections in dissipative CBFs may extend the fatigue life of hollow brace section members. Thus, the brace-gusset plate test specimens compare the performance of specimens designed using conventional methods with the proposed balanced design method.

The test frame (or 'mock-up') used for the BRACED experiments on the Azalee shake table was designed to facilitate the testing of multiple pairs of brace-gusset plate specimens, by allowing the specimens to be exchanged between experiments. The brace member and connection details were varied between experiments to investigate the range of global and local member slenderness found in European design practice, and to assess the effect of conventional and novel gusset plate designs. In each experiment, three separate earthquake tests were performed with table excitations scaled to produce elastic response, brace buckling and/or yielding and brace fracture. The principal outcomes included measurements of the displacement ductility capacity of the brace specimens; an evaluation of the influence of gusset plate detailing on connection ductility; observations on the contributions of brace and connection yielding to overall inelastic deformation of CBFs; measurements of equivalent viscous damping in CBFs; assessment and improvement of Eurocode 8 design guidance for CBFs; and validation of numerical models.

20.2.3 Shake Table Experimental Programme

The shake table experimental programme investigated the performance of CBFs at different levels of seismic excitation, including ultimate behaviour, through shake table testing of a model frame incorporating a pair of brace-gusset plate specimens. To address project objectives, three different test parameters were examined in these tests: brace cross-section size; brace connection configuration and gusset plate design. The following notation is used to identify the properties of the brace-gusset plate specimens examined in individual experiments:

Brace Section Size:
S1 80 × 80 × 3.0 SHS
S2 100 × 50 × 3.0 RHS
S3 80 × 40 × 3.0 RHS
S4 60 × 60 × 3.0 SHS
Connection Configuration:
CA Gusset connection to beam and column flange
CB Gusset connection to beam flange only
Gusset Plate Design:
G1 Conventional design with Standard Linear Clearance (SLC)
G2 Balanced design with Elliptical Clearance (EC)

The schedule of tests presented in Tables 20.1 and 20.2 was designed to address all of the above test parameters. In this table, the values for non-dimensional slenderness, λ_{nom}, are calculated assuming actual member cross-section areas, pinned-pinned boundary conditions with bending about the minor axis (K = 1.0) and both nominal (f_y = 235 MPa for braces; f_y = 275 MPa for gusset plates) and actual material yield strengths. The λ_{nom} values shown were selected to cover the range of brace slenderness allowed by Eurocode 8. The b/t values imply Class 1 cross-sections, as required for dissipative brace members, but the higher values are close to the boundary with Class 2 to capture the influence of local buckling on brace ductility. The β_{ww} parameter (Lehman et al. 2008) represents the ratio of the plastic tension resistances of the brace member and gusset plates. Specimens with conventionally designed gusset plates have low β_{ww} values, implying that gusset yielding will not occur, whereas those designed using the balanced design approach have higher β_{ww} values, implying that gusset yielding may occur.

A pair of identical brace-gusset plate specimens is tested in each experiment. A total of 12 experiments are included in the programme, and the test frame is designed to allow the brace-gusset plate specimens to be exchanged between experiments. To this end, the gusset plates are welded to flange plates which are bolted to the flanges of the beam and column members. All specimens were tested under uniaxial seismic excitation using the same earthquake record scaled to three different levels. The signal employed is a natural ground record from the PEER database, recorded in Imperial Valley (California, USA) during the 1940 earthquake. In each test, three levels of earthquake were examined: (i) low-level with elastic response, (ii) medium-level with brace buckling and yielding, and (iii) high-level with brace fracture. These are represented by earthquake events with

Table 20.1 Specimen properties: brace member

Test	Specimen	Section size	Brace length (mm)	Characteristic strength		Yield capacity		Non-dimensional slenderness		Buckling capacity	
				R_{eH} (MPa)	R_m (MPa)	$N_{pl, Rd}$ (kN)	$N_{pl, ck}$ (kN)	λ_{nom}	λ_{ck}	$N_{b, Rd}$ (kN)	$N_{b, ck}$ (kN)
1	S1-CA-G1	80×80×3.0	2413	372.5	437.0	214.8	340.8	0.83	1.04	167.6	217.3
2	S3-CA-G1	80×40×3.0	2427	384.3	430.5	158.4	259.0	1.59	2.03	53.6	56.3
3	S4-CA-G1	60×60×3.0	2425	347.5	404.0	158.4	234.2	1.11	1.35	93.0	103.4
4	S2-CA-G1	100×50×3.0	2413	341.5	377.7	200.7	291.6	1.24	1.49	102.0	110.0
5	S1-CA-G2	80×80×3.0	2502	337.8	389.0	214.8	308.7	0.86	1.03	163.6	199.7
6	S2-CA-G2	100×50×3.0	2509	341.7	380.2	200.7	291.8	1.28	1.55	96.2	102.9
7	S3-CA-G2	80×40×3.0	2504	370.5	429.7	158.4	249.7	1.64	2.05	50.8	53.0
8	S1-CB-G1	80×80×3.0	2395	336.5	388.8	214.8	307.6	0.82	0.98	168.4	208.7
9	S2-CB-G1	100×50×3.0	2395	340.0	377.8	200.7	290.4	1.23	1.48	103.1	111.3
10	S4-CB-G2	60×60×3.0	2437	347.5	404.0	158.4	234.2	1.12	1.36	92.4	102.6
11	S2-CB-G2	100×50×3.0	2433	341.5	377.7	200.7	291.6	1.25	1.50	100.7	108.4
12	S3-CB-G2	80×40×3.0	2420	370.5	429.7	158.4	249.7	1.58	1.99	53.9	56.4

Table 20.2 Specimen properties: gusset plate connection

Test	Specimen	Gusset type	t_p t_p (mm)	Characteristic strength		Yield capacity		Balance factor		Buckling capacity	
				R_{eH} (MPa)	R_m (MPa)	$N_{pl, Rd}$ (kN)	$N_{pl, ck}$ (kN)	$\beta_{ww, Rd}$	$\beta_{ww, ck}$	$N_{b, Rd}$ (kN)	$N_{b, ck}$ (kN)
1	S1-CA-G1	SLC	12	369.0	506.7	835.6	1121.2	0.33	0.28	737.5	941.4
2	S3-CA-G1	SLC	8	337.0	490.0	557.1	682.6	0.36	0.35	412.6	461.6
3	S4-CA-G1	SLC	8	337.0	490.0	513.1	628.7	0.39	0.36	370.5	411.4
4	S2-CA-G1	SLC	12	369.0	506.7	901.6	1209.8	0.28	0.23	804.8	1032.8
5	S1-CA-G2	EC	5	336.0	444.7	348.2	425.4	0.79	0.73	302.6	356.3
6	S2-CA-G2	EC	4	388.0	488.0	300.5	424.0	0.85	0.68	260.3	341.5
7	S3-CA-G2	EC	4	388.0	488.0	278.5	393.0	0.72	0.62	233.5	299.9
8	S1-CB-G1	SLC	12	369.0	506.7	835.6	1121.2	0.33	0.27	747.6	960.6
9	S2-CB-G1	SLC	12	369.0	506.7	901.6	1209.8	0.28	0.24	798.1	1020.2
10	S4-CB-G2	EC	4	388.0	488.0	256.5	361.9	0.79	0.64	126.0	134.6
11	S2-CB-G2	EC	4	388.0	488.0	300.5	424.0	0.85	0.69	140.7	149.5
12	S3-CB-G2	EC	4	388.0	488.0	278.5	393.0	0.72	0.62	109.1	114.1

50, 10 and 2 % probability of exceedance in 50 years respectively. Low-level white noise excitation was also applied before and after each earthquake level to monitor the evolution of elastic properties with brace member damage.

The spectrum of the input seismic signal was normalized to the lowest seismic level expected in the test sequence, namely a PGA of 0.1 g. This was considered to be the 0 dB level, and the signal was then amplified for different excitation levels. The original signal was filtered at low frequency to limit the maximum displacement under the ± 100 mm limit value for the AZALEE table. The high pass filter eliminated frequencies under 0.7 Hz. This filtering was also necessary to obtain a null value of table displacement at the end of the test. The signal duration was 40 s with five seconds at null value added at the beginning to provide time to check the correct triggering of the data acquisition system.

20.3 Test Frame and Specimens

20.3.1 Test Frame

The test frame was designed as a dedicated single-storey model CBF structure capable of accommodating the full range brace and gusset-plate connection specimens set out in Tables 20.1 and 20.2. These specimens were designed so that they could be tested to failure within the capacity of the shaking table. The following specific requirements drove the primary test frame geometry and strength specimen design:

- The test frame should have a realistic storey height and natural period
- The mass supported by the test frame should not exceed 50 t
- The PGA required to fracture the brace specimens should not exceed 1.0 g
- The displacement ductility demand required for brace fracture ($\mu_\Delta > 4$) should be accommodated by the test frame
- Brace lengths shall should be realistic; non-dimensional slenderness should be within or close to Eurocode 8 limits
- Braces members should possess class 1 cross-sections, but small b/t and d/t ratios should be avoided to ensure that local buckling and fracture is observed
- The brace- and gusset plate specimens should be easily exchanged between tests
- Brace connections to beam and column (CA) and beam only (CB) should be accommodated
- Two gusset plate designs should be included: conventional design (G1) with standard linear clearance (SLC) plastic hinge detailing, and balanced design (G2) with elliptical clearance (EC) plastic hinge detailing

These objectives were completed whilst remaining within the AZALEE shake table constraints described in the previous section. Figures 20.1 and 20.2 show the resulting design of the test frame. The lateral resistance of the frame was provided by a pair of brace specimens in Frame B which were positioned in the same plane

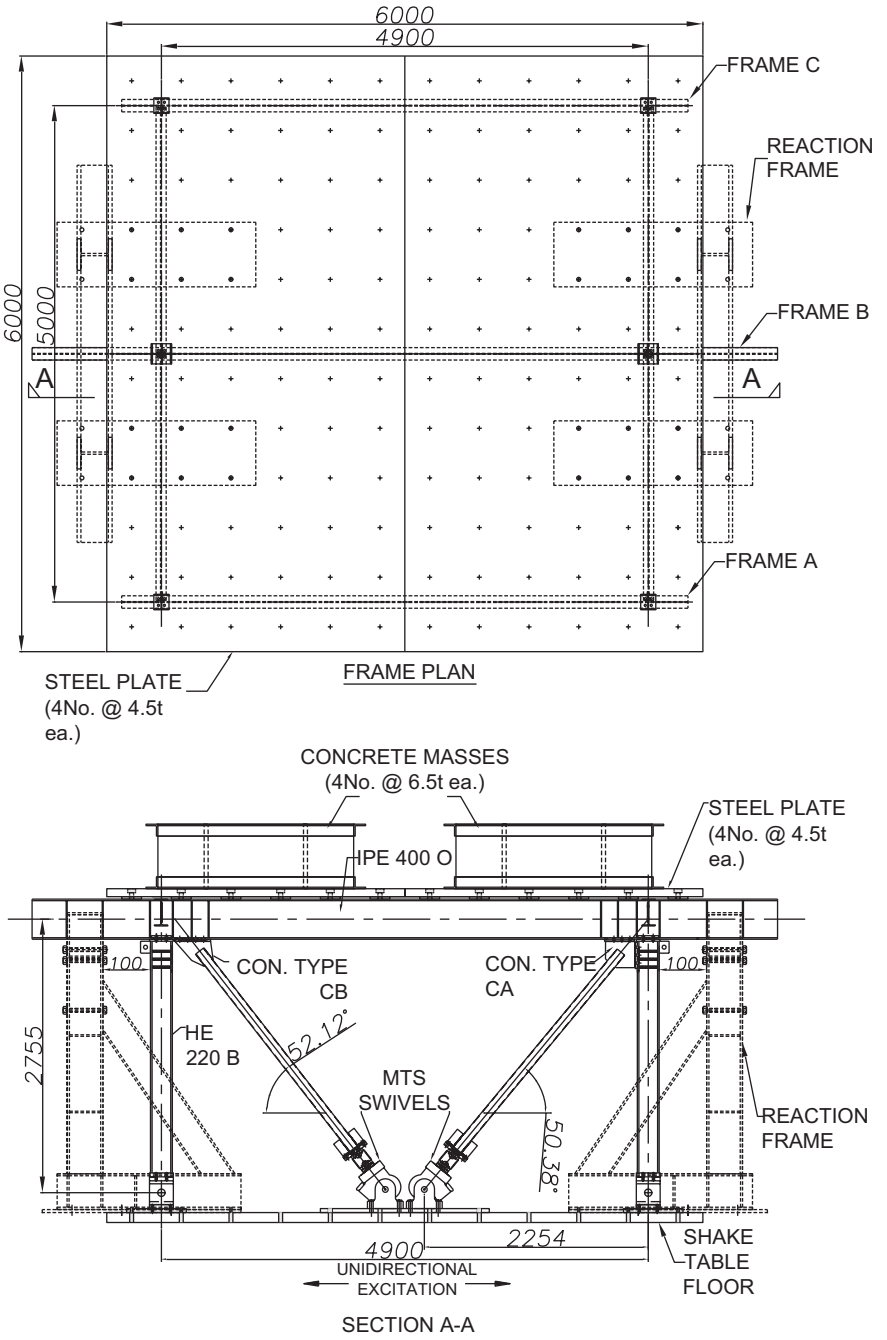

Fig. 20.1 Plan and elevation of BRACED test frame on Azalee platform. *CA* and *CB* connections shown for illustration, identical brace specimen pairs were used in all tests

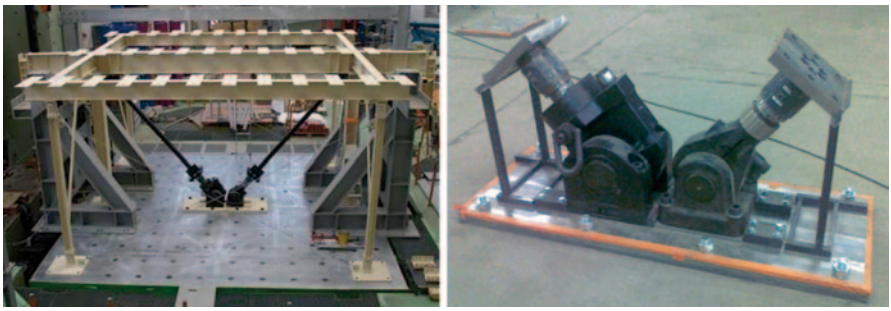

Fig. 20.2 Test frame without added masses and MTS swivel bearing with load cells

to prevent any significant torsional response. The test frame is symmetrical at either side of Frame B. Two additional unbraced frames (Frame A and C) were located on either side of the CBF model to provide lateral stability; lateral beams support the added mass of the frame. All column members in Frames A and C were pinned at the top and bottom ends. Columns in Frame B were pinned at their bottom ends and bolted connected at their top ends to the primary beam by a flush end plate bolted connection.

The principal elements of the test frame are:

- a main beam in Frame B (IPE 400), length 7500 mm
- two columns in Frame B (HE 220 B) supporting the IPE 400
- two columns each on Frames A and C (HE 120 A)
- six beams (IPE 270), forming a square horizontal roof grid, supported by the outer columns and fixed to the main IPE 400 beam in Frame B
- four transverse braces (100 × 20 mm solid cross-section) to provide lateral stability to the frame in the direction perpendicular to Frames A–C
- two MTS swivel bearings (described below) with load cells assemblies
- two brace members, which are the elements tested, mounted in the main plane between the swivels and the IPE 400/HE 220 angle
- two mechanical devices to return the frame to vertical plumb after each test

20.3.2 Brace-Gusset Plate Specimens

Twenty-four identical brace tube pairs were designed using four different cross-section sizes for two connection types (CA and CB) and two gusset plate types (G1 and G2). The yield and buckling capacities (based on nominal and measured steel strengths) are presented in Tables 20.1 and 20.2. The corresponding non-dimensional slenderness is also presented. The area used for the calculation of brace resistance is the product of the Whitmore width and the gusset plate thickness t_p. Two connection design approaches were applied to each of the four brace cross-section sizes and the two connection types, CA and CB (Fig. 20.3). These are conventional designs using

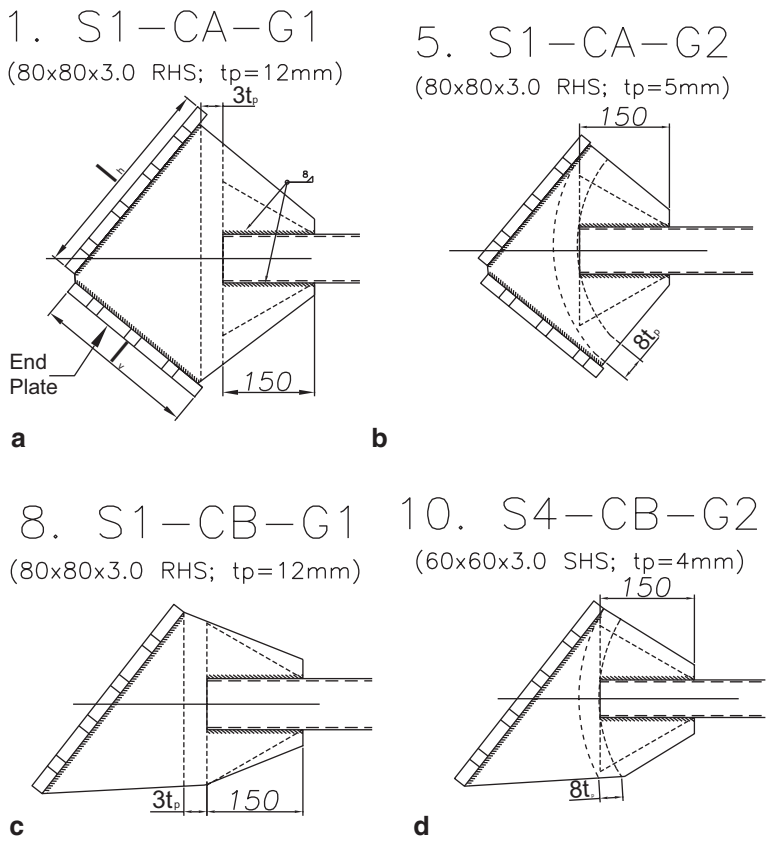

Fig. 20.3 Sample gusset plate connection designs **a** CA-G1 **b** CA-G2 **c** CB-G1 and **d** CB-G2

the standard linear clearance detailing rule for the gusset plate and balanced design using the elliptical clearance detailing rule (Lehman et al. 2008).

The concept of balancing the brace tensile yielding and gusset yielding mechanisms has been encapsulated using the balance factor β_{ww}. The conservative nature of the G1 gusset designs resulted in low (~0.2–0.3) β_{ww} values. A higher range of β_{ww} values (~0.6–0.75) was achieved for the G2 designs by specifying thinner gusset plates and employing the more compact EC detailing rather than the SLC detailing used in the G1 specimens. For all G1 specimens a linear plastic hinge clearance length of $3t_p$ was used while an elliptical clearance zone of thickness $8t_p$ was used for the G2 plastic hinge. Values for expected yield stress ratio R_y were used to calculate $\beta_{ww,\,Rd}$ values, while characteristic material strengths were used to calculate values of $\beta_{ww,\,ck}$.

20.4 Experimental Results

A wide range of response variables were measured in each test, including table and response (roof) accelerations and displacements, brace elongation and axial force, and strains in the brace member and gusset plate. Figure 20.4 presents a sample of some of the recorded results from the final run in Test 4, where brace fracture occurred after approximately 30 s after the test had been completed.

Brace fracture was observed in all tests, either in the third or fourth earthquake exciation run. During the low level test excitations the frame remained elastic with no brace buckling. Brace buckling and yielding occurred in the intermediate level runs, sometimes with large out-of-plane brace buckling deformations, but always limited plastic deformation demand. A fully inelastic response was observed in all high level excitation tests, usually causing fracture in one or both braces. In some tests, an additional failure level earthquake excitation run was added to cause brace fracture. A similar pattern of failure was displayed in most cases: brace buckling in compression led to large out-of-plane brace bending and the formation of a plastic

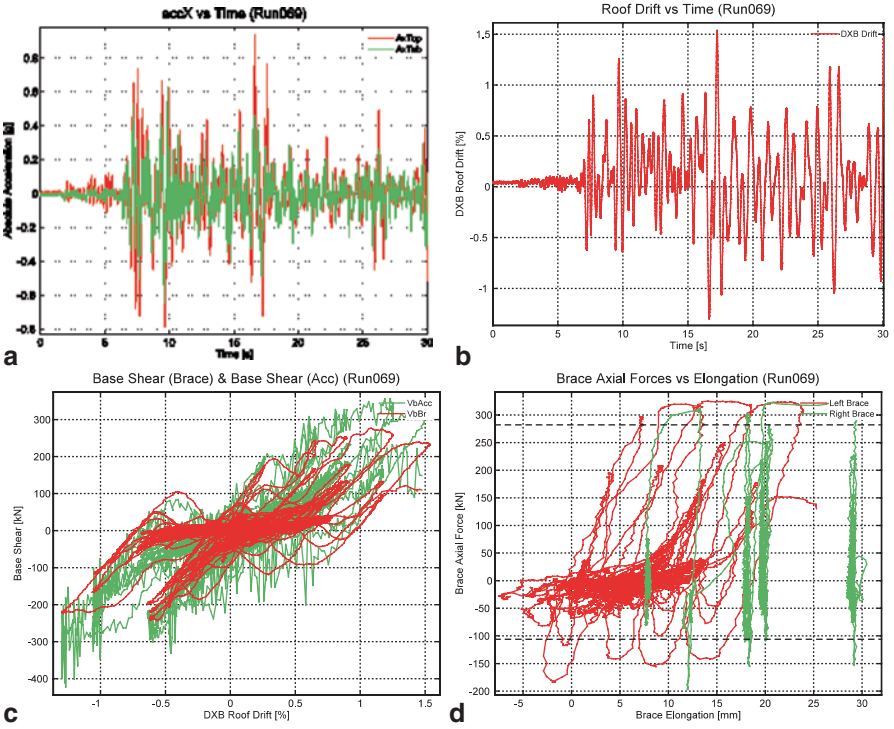

Fig. 20.4 Measured response in Test 4: **a** table and response accelerations; **b** Frame storey drift; **c** Base shear-drift hysteresis; **d** brace force-elongation hysteresis

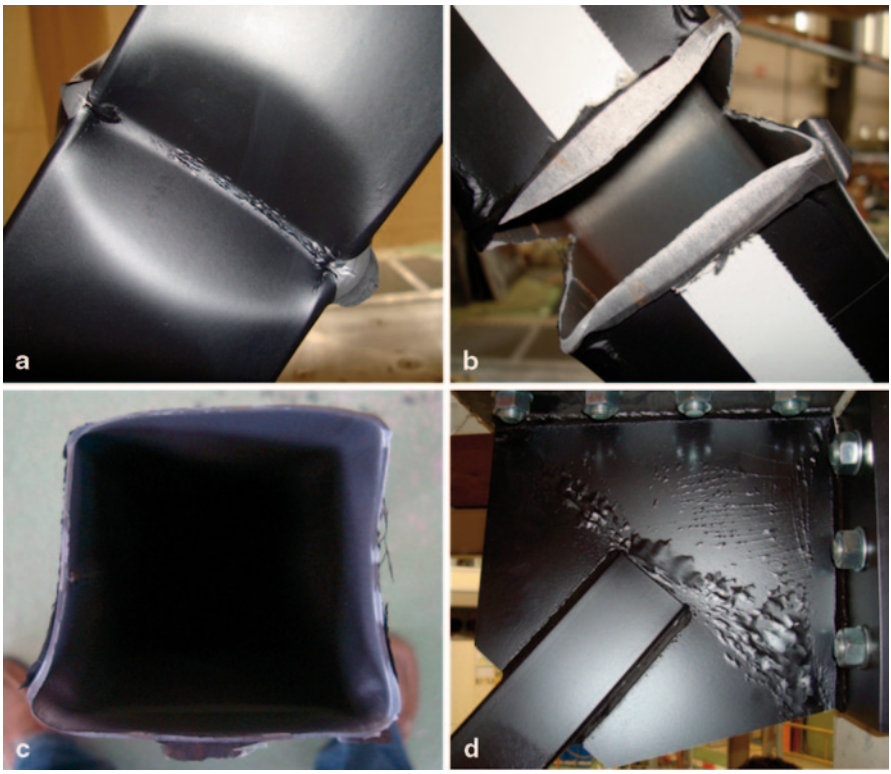

Fig. 20.5 Images of specimen deformation and fracture. **a** local buckle at brace mid-length with initial tear; **b** incomplete fracture of brace; **c** deformed shape of brace cross-section after local buckling and fracture; **d** yield pattern in gusset plate with SLC detail

hinge close to brace mid-length. During large amplitude displacement cycles, local buckling occurred in these plastic hinges, and as the hinge rotation demand increased, a small tear would initiate at the peak of the local buckle. Upon subsequent reversal of the direction of frame response the brace experienced tension forces which caused these tears to propagate throughout the depth of the cross section causing brace fracture. Figure 20.5 presents a set of images from different tests that illustrate this process. Also shown is a gusset plate after testing, displaying a yield pattern in the plastic hinge that must form in the gusset plate to accommodate large out-of-plane brace buckling deformations. No gusset plate failures (plate fracture, plate buckling, weld or bolt failure) occurred in any of the tests, validating the capacity design and overstrength procedures employed (AISC 2005; CEN 2004).

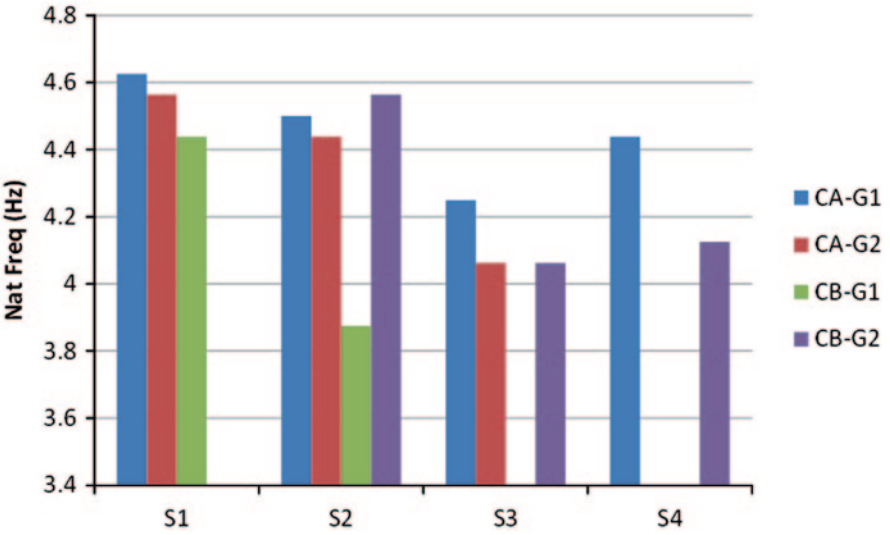

Fig. 20.6 Initial natural frequency of test frames by specimen characteristics

20.4.1 Frame Stiffness

Figure 20.6 compares the initial natural frequency of each test by brace specimen cross-section size and gusset plate connection configuration. The values vary in a relatively narrow range between 3.8 and 4.6 Hz approximately. The larger cross-sections (S1 and S2) tend to display higher natural frequencies than the smaller ones (S3 and S4), but not in every case, and the differences are less than the differences in brace cross-section area. For a given cross-section size, the highest natural frequency (and therefore frame stiffness) tends to be displayed by specimens with the conventional CA-G1 connection configuration, but the reductions in natural frequency observed with other configurations are small.

Figure 20.7 examines the evolution of frame natural frequency in each individual test, grouped by brace-gusset specimen cross-section size. In Fig. 20.7a the natural frequency of the frame with S1 cross-sections does not reduce much between the initial and final runs because the maximum drift demand (in the 10% probability of exceedance in 50 years earthquake test run) remained less than 1%, and the brace had not experienced large out-of-plane buckling deformations. In contrast, Fig. 20.7b–d display large reductions in natural frequency after subsequent runs (10 and 2% probability of exceedance in 50 years where additional failure level earthquake runs were executed). The S2, S3 and S4 cross-section sizes in these specimens lead to larger out-of-plane brace buckling slendernesses, and larger brace buckling deformations.

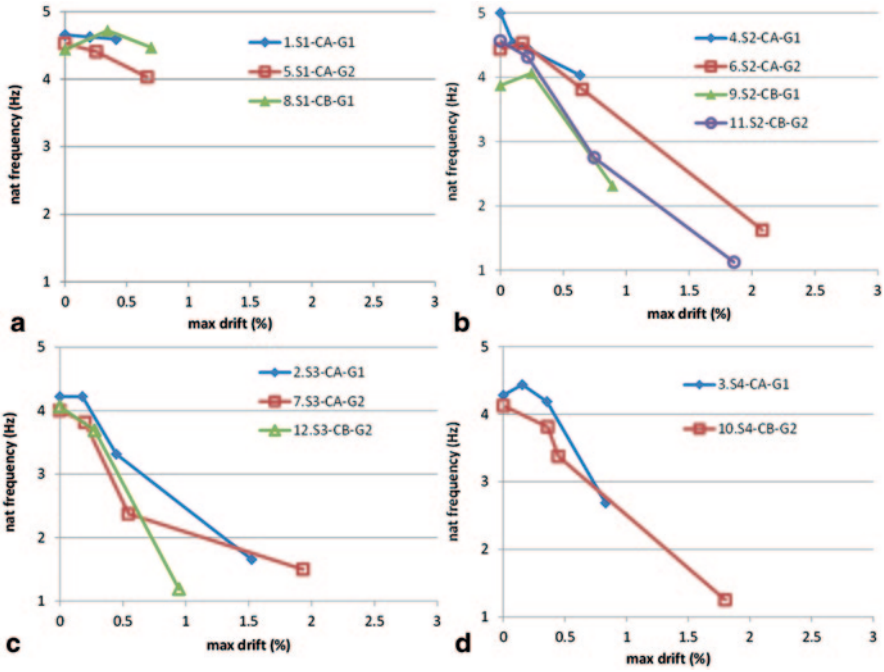

Fig. 20.7 Evolution of natural frequency with previous maximum drift demand in individual tests by brace-gusset plate specimen cross section. **a** S1 brace cross-sections, **b** S2 brace cross-sections, **c** S3 brace cross-sections, **d** S4 brace cross-sections

20.4.2 Frame Drift and Brace Ductility

Figure 20.8 compares the variation in maximum drift demand with the PGA displayed in each test. The results are grouped by brace-gusset plate specimen cross-section size. The larger cross sections (S1 and S2) display a mostly linear relationship between drift and PGA, while the smaller cross sections (S3 and S4) exhibit increasing drift values for higher PGA. This behavior may be expected in short period structures that are subjected to ground excitations substantially greater than those required for initial yield.

Measured maximum frame drift and brace force data can be combined to give a high-level indication of the influence of brace-gusset plate specimen connection type on the global ductility capacity of the test frame. The design of the experimental programme provided pairs of tests in which the specimens differ in only one of the main test variables (brace cross-section, connection type and gusset plate design). Figure 20.9 compares the response of pairs of tests which both employed the same brace cross-section, but different connection details. The plots shown compare the variation in the maximum normalized brace force observed in each run with the maximum drift experienced by the test frame in that run. Three plots compare the

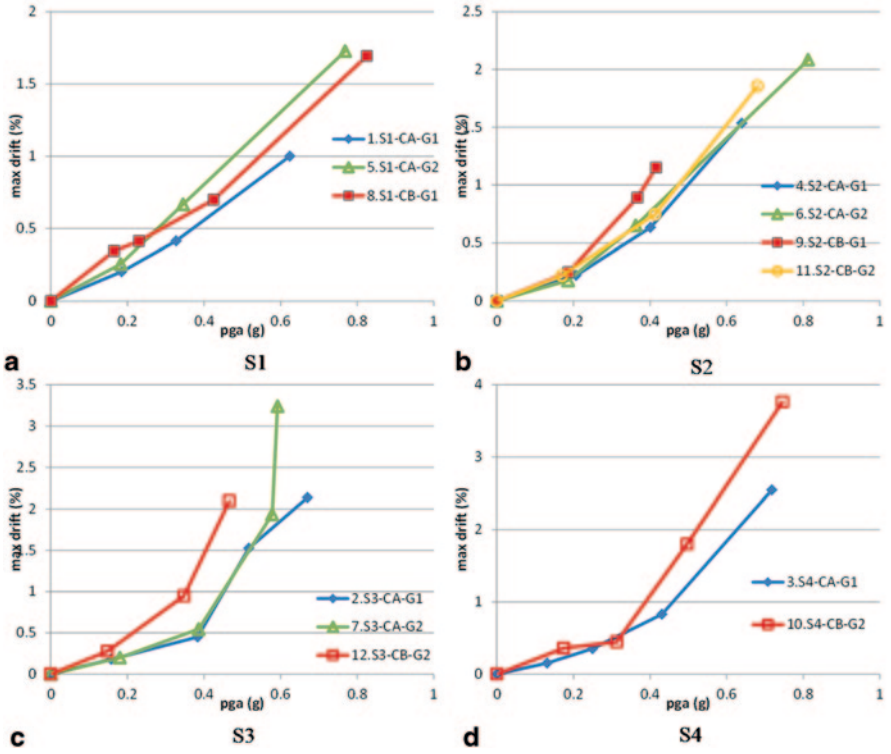

Fig. 20.8 Variation of maximum storey drift demand with PGA by specimen cross section

application of the conventional and balanced design methods to CA-type connections. In each case, the balanced design reaches a larger drift before brace fracture. This is especially noticeable with the 80 × 80 specimens in which the conventional design experienced brace fracture at a drift of only 1 %. The maximum brace forces are also greater in the balanced design cases. Overall, the comparisons presented in Fig. 20.9 support the hypothesis that the use of the balanced gusset plate design method leads to a more ductile and dissipative response in CBFs without loss of brace resistance.

Figure 20.10 presents the observed displacement ductility capacity of the brace-gusset plate specimens. The brace ductility capacity values shown are obtained by normalizing the brace fracture elongation by the brace yield displacement. The brace fracture elongation is the maximum measured change in overall brace length in a fractured brace during the earthquake test run in which that brace fractured. This change in length may be an increase in length (elongation under tension) or a reduction in length (shortening under compression) and includes the effects of axial deformations in the tube length and gusset plate strains. The brace yield displacement is obtained by multiplying the length of the unstiffened brace tube by its char-

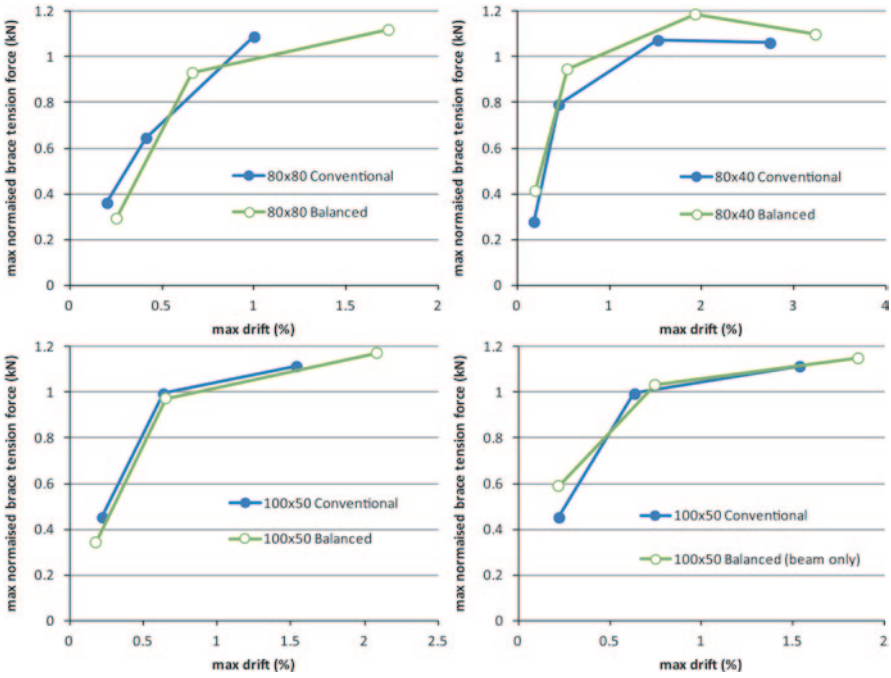

Fig. 20.9 Variation of maximum storey drift demand with PGA by specimen cross section

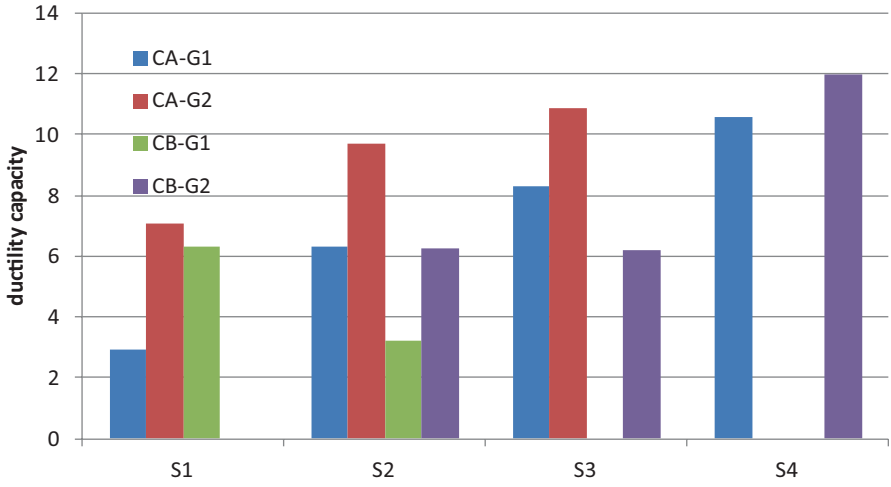

Fig. 20.10 Brace displacement ductility capacity by specimen characteristics

acteristic yield strain, identified from the results of the characteristic steel strengths presented in Tables 20.1 and 20.2.

The measured brace displacement ductility capacities vary between 2.9 and 12.0, with a mean value of 7.5. The variation between the values identified in each test is attributable to the main test specimen parameters: member slenderness, cross-section slenderness, connection type and gusset plate design method. Larger ductility capacities were displayed by more slender specimens with smaller cross sections (S3 and S4), and the use of the balanced gusset design approach (G2) leads to larger brace ductility capacity than the conventional approach (G1). In the four cases where direct comparison between specimens designed using these two approaches can be made, the improvement ranges from 30–140 %, with a mean improvement of 80 %.

20.5 Conclusions

The BRACED project completed a series of shake table tests on a model CBF employing various brace members with different cross-section and gusset plate connection details. Amongst other properties, the test results identified the evolution of frame stiffness with drift level, the sensitivity of frame drift to PGA level, and the brace displacement ductility capacity displayed with different brace member-gusset plate combinations. In particular, the tests confirmed that the use of a balanced design approach in which gusset plate and brace member resistances are designed to ensure a more uniform distribution of plastic strains can lead to higher brace ductility capacities.

The experimental results can also be used to validate and improve empirical models for the ductility capacity of hollow section bracing members, identify active yield mechanisms and failure modes in different brace member/connection configurations, develop and validate numerical models for simulating the inelastic seismic response of CBFs, and provide essential data on the earthquake response of European CBFs.

Acknowledgements The research leading to these results received founding from the European Community's Seventh Framework Programme [FP7/2007–2013] for access to the TAMARIS laboratory in CEA/Saclay, France under grant agreement n 227887.

References

AISC (2005) ANSI/AISC 341-05 Seismic provisions for structural steel buildings. American institute of steel construction, Chicago, Illinois

CEN (2004) EN 1998-1:2004, Eurocode 8: Design of structures for earthquake resistance—Part 1: general rules, seismic actions and rules for buildings. European committee for standardization, Brussels, Belgium

Elghazouli AY (2003) Seismic design procedures for concentrically braced frames. Struct Build 156:381–394
Goggins JM, Broderick BM, Elghazouli AY, Lucas AS (2006) Behaviour of tubular steel members under cyclic axial loading. J Constr Steel Res 62:121–131
Lehman DE, Roeder CW, Herman D, Johnson S, Kotulka B (2008) Improved seismic performance of gusset plate connections. J Struct Eng 134:890–901
Nip KH, Gardner L, Elghazouli AY (2010) Cyclic testing and numerical modelling of carbon steel and stainless steel tubular bracing members. Eng Struct 32:424–441
Popov EP, Black RG (1981) Steel struts under severe cyclic loadings. J Struct Div, ASCE 107(7):1857–1881
Tremblay R (2002) Inelastic seismic response of steel bracing members. J Constr Steel Res 58:665–701